General picture of co-nonsolvency for linear and ring polymers

Gyehyun Park, Eunsang Lee† and YounJoon Jung*

Department of Chemistry, Seoul National University, Seoul 151-747, Korea
Received 2nd March 2016; Accepted Date (to be inserted by the publisher after your manuscript is accepted)

Co-nonsolvency is a puzzling phenomenon that a polymer swells in a good solvent individually, but it collapses in a mixture of good solvents. This structural transition with changing solvent environment has been drawing attention due to practical application for stimuli-responsive polymer. The aim of this work is to describe the physical origin of the co-nonsolvency. In this work, we present Monte Carlo simulations for polymer solutions by using simple and general model. We simulate linear and ring polymers to compare their co-nonsolvency behaviors. Calculating Flory exponents and bridging fractions gives a good description for polymer structures. While the polymer structure shows non-monotonous behavior with increasing the cosolvent fraction, the chemical potential decreases monotonously. This indicates that coil-to-globule transition of polymers is purely controlled by free energy and can be regarded as a thermodynamics transition. We also present that ring polymers have higher looping probability than linear polymers, thus the bridging fraction remains higher at high cosolvent fraction. Our study provides a new perspective to understand polymer structure when the polymer "dissolves well" in any solvent.

Keywords: Co-nonsolvency, coil-globule-coil transition, ring polymer, bridging fraction, adsorption model

Introduction

Smart polymer often referred to a stimuli-responsive polymer whose structures and functions respond to physical and chemical stimuli such as temperature, humidity, pH, solvent quality, etc. It has been drawing much attention in recent years due to its practical applications ranging from bio-technology to material science.[1,2,3,4] Drug transportation is a representative example of such smart polymer applications. An insulin-dependent diabetic needs insulin with increasing internal glucose concentration. An insulin carrier made of smart polymers changes its structure to release insulin by detecting glucose molecules inside a patient's body. However, physics of such smart polymers linked with chemical stimuli is still a theoretically challenging problem, while thermo-responsive polymers have been well understood by a number of researchers.[3,4] Since the temperature of human body is almost constant, it is highly desired to understand the structural behavior of polymers under changing chemical environment.

Solvent quality is one of well-known stimuli for a stimuli-responsive polymer. The idea that solvent quality controls the polymer structure has been traditionally accepted, such that good solvent makes the polymer swell and a poor solvent makes it collapse. It is recently shown that, however, such theoretical framework breaks when a polymer is solvated in mixed good solvents. One experimental study reported that a lower critical solution temperature (LCST) of poly-N-isopropylacrylamide (PNIPAm) changes non-monotonically in mixed water/methanal solvent with increasing the methanol fraction.[5] This finding supported an interesting coil-globule-coil transition in the mixed solvent even if two solvents are both good. It is usually called co-nonsolvency. In order to understand physics behind this abnormal transition, Flory-Huggins type[5,7] and hydrogen-bonding arguments[6,8] have been provided. Most fascinating approach for this behavior was asserted by Mukherji, which is a general bridging scenario of a cosolvent molecule between two monomers.[9,10,11] An effect of such local density fluctuation was modeled by an adsorption argument with additional free energy penalty for polymer looping, which plays a central role in the globule-coil reentrance. It is also interesting to note that coil-globule transition with adding small fraction of cosolvent is first order-like transition, while globule-coil transition is continuous.

According to the argument above, polymers with other topologies such as ring and branched polymers are expected to show distinct co-nonsolvency behaviors due to different free energy penalties for looping. Especially, a ring polymer has no chain end resulting in higher looping probability than linear counterpart. Its topological effects on the structure have been intensively studied ranging from a dilute solution to a concentrated melt.[12,13,14,15,16,17] Although half of the ring follows a self-avoiding walk (SAW) in a good solvent, the

topology of connected ends leads to the high integrated looping probability. Moreover, its potential application as a smart polymer has been spotlighted since recent experiments synthesized and purified the ring polymers.[17] In this study, therefore, we provide a general picture of ring polymer co-nonsolvency using Monte-Carlo simulations of off-lattice bead-spring model. The adsorption argument is also applied to ring polymers to explain our results.

This paper is organized as follows. We first explain details of our model and simulation methods. After providing simple theories for polymer and liquid systems to apply them to our arguments, we show the results including polymer sizes, bridging fractions, and chemical potentials of a polymer as a function of cosolvent fraction. To clarify the structure in each condition, we also present radial distribution functions and single molecule structure factors. Concluding remarks follows in the final section.

Theory and Computational Method

In this work, we use coarse-grained bead-spring model and spherical solvent molecules similar with Ref 6.[9,18] First, a polymer is composed of spherical beads connected by harmonic potential. Each bead represents a Kuhn monomer and the non-bonded interaction between two monomers are modeled by repulsive Lennard-Jones potential, such that:

$$V_{LJ}(r) = \begin{cases} 4\epsilon_m \left[\left(\frac{\sigma_m}{r}\right)^{12} - \left(\frac{\sigma_m}{r}\right)^{6} + \frac{1}{4} \right] & \text{for } r \le 2^{1/6}\sigma \\ 0 & \text{elsewhere,} \end{cases} \quad (1)$$

with ε_m=1.0ε and σ_m=1.0σ, where ε and σ is a unit energy and a unit length, respectively. Two bonded monomers are excluded for this non-bonded interaction, but those are connected by a harmonic bond, such that:

$$V_{harmonic}(r) = \frac{1}{2}k(r-\sigma_m)^2. \quad (2)$$

We use a large force constant of k=100.0ε/σ^2 to prevent bond-crossing event during simulations. Two kinds of solvents are used to fill up the polymer system, and both mimic well-mixed polymer solution systems. One kind of solvent molecules (later termed a good solvent, GS) solvate a polymer well, and the non-bonded interaction between a monomer and a good solvent is modeled by repulsive Lennard-Jones, such as:

$$V_{LJ}(r) = \begin{cases} 4\epsilon_{mg} \left[\left(\frac{\sigma_{mg}}{r}\right)^{12} - \left(\frac{\sigma_{mg}}{r}\right)^{6} + \frac{1}{4} \right] & \text{for } r \le 2^{1/6}\sigma_{mg} \\ 0 & \text{elsewhere,} \end{cases} \quad (3)$$

where ε_{mg}=1.0ε and σ_{mg}=0.75σ. Another kind of solvents is also good (termed a better solvent or cosolvent, *BS*) modeled by the shifted Lennard-Jones potential between a solvent and a monomer, such that:

$$V_{LJ}(r) = \begin{cases} 4\epsilon_{mb} \left[\left(\frac{\sigma_{mb}}{r}\right)^{12} - \left(\frac{\sigma_{mb}}{r}\right)^{6} - \left(\frac{\sigma_{mb}}{r_c}\right)^{12} + \left(\frac{\sigma_{mb}}{r_c}\right)^{6} \right] & \text{for } r \le 2.5\sigma \\ 0 & \text{elsewhere,} \end{cases} \quad (4)$$

where ε_{mb}=1.0ε and σ_{mb}=0.75σ. Attractive force between the better solvent and a monomer plays a critical role in co-nonsolvency. Three solvent pairs of GS-GS, BS-BS, and GS-BS are represented by the same repulsive Lennard-Jones potential of Eqn. (1), but with ε_{ij}=1.0ε and σ_{ij}=0.5σ. It is important to note that a polymer in good solvents is modeled by only repulsive potentials, but a swelling configuration of a polymer is entropically favored at a finite temperature.

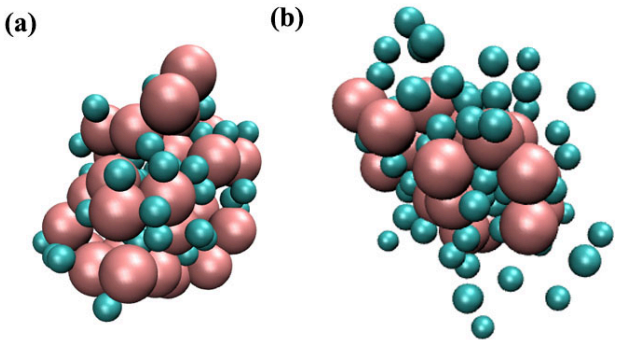

Figure 1. Simulation snapshots of N_l=30 ring polymers at cosolvent fraction (a) x_c=0.1 and (b) x_c=0.9. Beads colored by red and blue represent a monomer and a cosolvent, respectively. For clarity, contacting cosolvent molecules on the polymer are only depicted.

Monte-Carlo simulation is employed to sample NVT trajectories of polymer solutions. After randomly choosing a particle, we try to move it with the maximum displacement of 0.5σ using the classical Metropolis algorithm. This maximum distance guarantees no bond-crossing event between polymer segments in our simulation temperature, T=0.5ε/k. We performed simulations for two topologically different polymers, linear and ring polymers, with the number of Kuhn segments N_l=10 and 30. The polymer is solvated by 2.5×10^4 solvent molecules. For each polymer case, we simulate eleven different solvent compositions ranging from x_c=0.0 to 1.0 at an interval of 0.1. The size of cubic box L is chosen to the average pressure being 40ε/σ^3,

so that L=22.0σ. Periodic boundary condition is used in all directions. Each system is equilibrated during 1.0×10^4 Monte Carlo steps (MCS) and all simulation results are analyzed from production runs during 1.0×10^4 MCS. Figure 1 shows simulation snapshots of our systems.

Results and Discussion

In order to verify our results, we first calculate radius of gyration of linear polymers of N_l=30 as a function of cosolvent fraction. An experimental result for PNIPAm in water/methanol mixed solvent is also plotted with our simulation results in Fig. 2(a).[19] In addition, normalized radius of gyration by its value at x_c=0.0 for four different polymer systems are also depicted in Fig. 2(b). All of these results show that our simulations reproduce coil-globule-coil transition as well as experiments and other simulation studies. It clearly shows the first order-like transition at x_c=0.0~0.1. With increasing cosolvent concentration, polymer slowly swells which is also well consistent with previous studies. In this figure, one can find that linear polymers contract much rapidly than ring polymers when a small number of cosolvents are added.

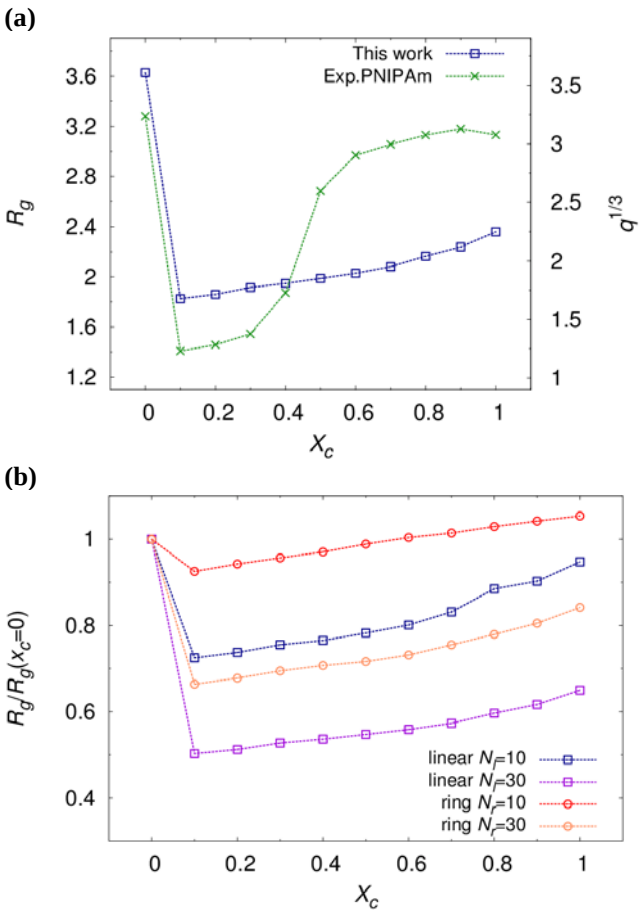

Figure 2. Radius of gyration R_g as a function of cosolvent molar fraction x_c. (**a**) Radius of gyration of linear polymer with chanin length N_l=30. For comparison, we include experimental data obtained from the degree of volume swelling ratio q for PNIPAm. (**b**) Normalized radii of gyration $R_g/R_g(x_c=0)$ as function of cosolvent molar fraction x_c is shown.

Observing detailed structures of polymers is essential to discuss the coil-golbule-coil transition as a function of cosolvent fraction. To do so, we briefly explain the simple theories for polymer structures in good and poor solvents. It is very instructive to introduce the concept of an excluded volume of a monomer, which is determined by effective interaction between two monomers, such that:

$$v_{\mathrm{ex}} = -\int d\mathbf{r}\,\exp[-u_{\mathrm{eff}}(r)/kT] - 1 \qquad (5)$$

Here, $u_{\mathrm{eff}}(r)$ is a effective potential between two monomers as a function of distance between them, r, k is Boltzmann constant and T is system temperature. The positive excluded volume means that two monomers feel effectively repulsive force, thus if the polymer is in a good solvent then $v_{\mathrm{ex}}>0$. The negative v_{ex} reflects the effective attraction between two monomers, which is the case of a polymer in a poor solvent. It is important to note that the excluded volume depends not only on the solvent quality but the temperature. The condition of $v_{\mathrm{ex}}=0$ is usually called θ-condition (θ-solvent and θ-temperature), and linear polymers follow ideal statistics in this condition.

To find the scaling relation between the mass and the size of polymers in a good solvent, we construct a free energy as a function of polymer size, R, and degree of polymerization, N. We first consider entropy of the chain as chain extension. If the chain is ideal, the probability of the size of end-to-end vector, purely originated from entropy, is Gaussian (~exp[-R^2/2Nb^2]), where b is Kuhn length. Therefore, free energy penalty for chain stretching is proportional to $kTR^2/2Nb^2$. Because the excluded volume of a monomer is positive, there is an energetic penalty for overlapping monomers. The probability that a monomer with an excluded volume v_{ex} overlaps with other monomers in the same polymer is proportional to $v_{\mathrm{ex}}N/R^3$. Since there are N monomers in a single polymer, total energetic contribution can be written as $kTv_{\mathrm{ex}}N^2/R^3$. The free energy of a polymer in a good solvent is given by:

$$F(R,N) = kT\left(\frac{R^2}{2Nb^2} + v_{\mathrm{ex}}\frac{N^2}{R^3}\right). \qquad (6)$$

Minimizing it with respect to R gives the relation between R and N, such that:

$$R \sim v_{\mathrm{ex}}^{1/5} b^{2/5} N^{3/5}. \qquad (7)$$

This approach is called Flory theory for SAW polymers and the scaling exponent for N is referred to Flory exponent, ν.[20] More sophisticated calculation using renormlization group theory gives ν=0.588. Calculating Flory exponent for polymers in a poor solvent is much straightforward. Since it is highly collapsed, we can imagine a large sphere including all monomers of a polymer without any empty space. In this case, mass of the system is proportional to cube of size, which leads to $R \sim N^{1/3}$.

Single molecule structure factor is the most efficient way to calculate Flory exponent not only in experiment but also in theoretical studies. It is usually calculated by:

$$S(\mathbf{q}) = \frac{1}{N}\sum_{i=1}^{N}\sum_{j=1}^{N} < \exp[-i\mathbf{q}\cdot\mathbf{r}_{ij}] > , \qquad (8)$$

where $\mathbf{r}_{ij}$ is a bond vector between two monomers in a single polymer. It is well known that $S(q)=N$ where $<R_g>q<1$ and $S(q)\sim q^{-1/\nu}$ where $1/<R_g> < q < 1/b$. Figure 2 shows single molecule structure factors for linear and ring polymer in x_c=0.0 and 0.1 conditions. One can find that for both linear and ring polymer cases, pure good solvent makes the polymer swells with the expoenent ν=3/5. At x_c=0.1, $S(q)\sim q^{-3}$ strongly indicates the collapsed polymer structures. For a swollen ring polymer, slight change of the exponent at q=1 is caused by its topology of connected chain end.

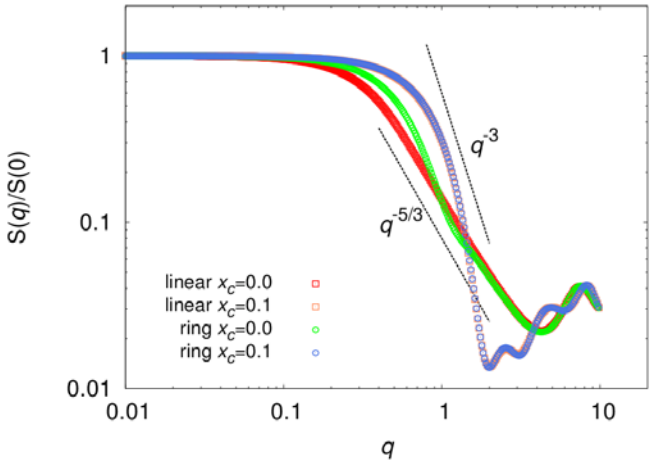

Figure 3. Normalized structure factors S(q)/S(0) for linear and ring polymer with a chain length N_l=30 in different cosolvent fraction, x_c=0.0 and 0.1. Squares and circles represent linear and ring polymer results, respectively. Different colors means different cosolvent concentrations and two scaling lines of ν=3/5 and 1/3 are drawn to guide an eye.

It has been recently known that such a rapid change in structure is closely linked to the bridging between a better solvent and monomers. Bridging structure means that a better solvent molecule connects two separating monomers in space due to their strong attractive force. In mixed good/better solvent condition, two contributions compete each other-one is entropically favored swollen structure and the other is energetic contribution which maximize the number of bridging cosolvents. When the number of better solvents is small, energy dominates over the entropic penalty for adsorption of cosolvent on the polymer backbone, which leads to the collapsed structure. With increasing the better solvent fraction, the entropic penalty increases and the polymer slowly reentrants into swelling regime. Figure 4(a) shows bridging fraction of as a function of cosolvent fraction. Here, we define a contact between a monomer and a cosolvent such that the distance between is closer than $2^{1/6}\sigma_{mb}$. And then, we also define the bridging fraction by the number of cosolvent molecules contacting with two separating monomers divided by the total number of interacting sites on polymer backbone. In both polymers, the bridging fraction has a maximum value at x_c=0.1~0.2, and again decreases as x_c increases. This is well consistent with the argument above and the results of gyration radii which the smallest in this concentration (Fig. 2(b)). It is also noteworthy that the bridging fraction of rings decreases slightly slower than linear polymers with increasing x_c, which is closely related to the looping probability.

(a)

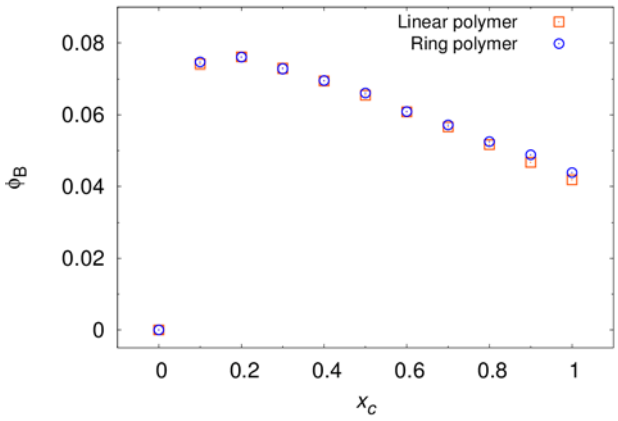

(b)

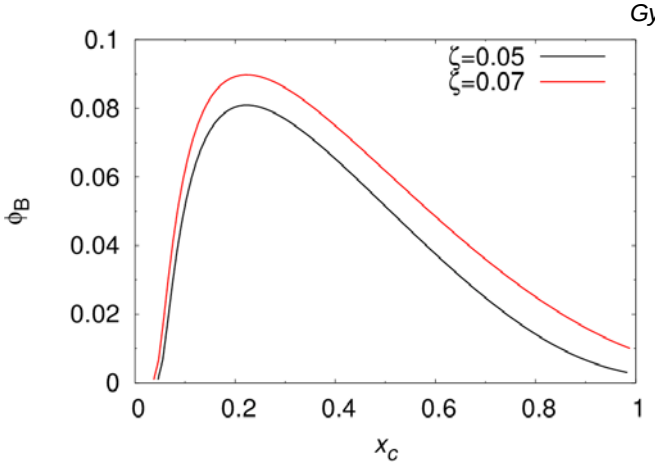

Figure 4. Bridging fraction as a function of cosolvent fraction. (a) Simulation results for linear (squares) and ring (circles) polymers. (b) Analytical solution for bridging fractions.

Such local fluctuation of better solvent concentration can be taken into account by the modified adsorption model proposed by Mukherji. In this model, N interaction sites on polymer backbone are occupied by three types of solvent molecules, a bridged cosolvent, a cosolvent and a good solvent, which fractions are written as φ_B, φ_C, and 1-φ_B-φ_C, respectively. The free energy of solvent adsorption can be written by:[9]

$$\begin{aligned}\frac{F}{kT} &= \phi_C \ln(\phi_C) + 2\phi_B \ln(2\phi_B) \\ &+(1-\phi_C-2\phi_B)\ln(1-\phi_C-2\phi_B) \\ &-E\phi_C - E_B\phi_B - \frac{\mu}{kT}(\phi_C+\phi_B)\end{aligned} \quad (9)$$

First three terms consider entropy for adsorption and next two terms includes interaction energy between cosolvents and polymers. Last term is for considering chemical potential of cosolvents calculated by μ=kTln(x_c). E and E_B are adsorption energies for non-bridged cosolvents and bridged cosolvents. Here, E_B=2E-E_{loop} where E_{loop} is free energy penalty for making loop, and E_{loop}=$m$ln(1/φ_B). By minimizing Eqn. (9) with respect to φ_C and φ_B, relation between φ_B and x_c can be obtained, such that:

$$\begin{aligned}16\phi_B^2 x_c &= x_c^*\Bigg\{\left(\frac{x_c^*}{x_c^{**}}\right)^{1/2}\phi_B^{m/2}(1-2\phi_B) \\ &\pm\sqrt{\left(\frac{x_c^*}{x_c^{**}}\right)\phi_B^m(1-2\phi_B)^2 - 16\phi_B^2}\Bigg\}^2,\end{aligned} \quad (10)$$

where x_c^*=exp(-E) and x_c^{**}=exp(-E_B). Figure 4(b) shows analytic solutions for above equation with ζ=2-m=0.05 and 0.07. Small value of m indicates small free energy penalty for looping, in turn, resulting in the high bridging fraction in large x_c. It shows a good agreement with our result that rings have higher looping probability than linear polymers, thus the bridging fraction remains higher at large x_c.

Radial distribution function between a monomer and a better solvent, $g_{mb}(r)$, supports the fact that the collapsed structure is originated from the strong attraction between this pair. Figure 5 shows $g_{mb}(r)$ for linear and ring polymer systems, and both give very similar results. For x_c=0.1, the first peak is very high, which means that the number of better solvents directly interacting with a polymer backbone is large. It is interesting to note that at this condition, better solvents are located not only in the first solvation shell but also in the region close to the polymer. In this context, it is again validated that the co-nonsolvency can not be understood by mean-field approach, but by the local density concentration of better solvents. Moreover, coil-to-globule transition by adding the small number of better solvents is energetically favored phenomenon. Therefore, we expect that large difference of attraction strengths between good solvent-monomer and better solvent-monomer leads to the co-nonsolvency behavior. It is shown that the peak height gradually decreases as well as the bridging fraction with increasing x_c. In this case, energetic contribution can be maximized by increasing φ_C and decreasing φ_B, thus the fraction of directly solvating cosolvents diminishs. Figure 6 shows pair distribution function between a monomer and a good solvent, $g_{mg}(r)$. The number of good solvents in the first solvation shell is anti-correlated with that of better solvents.

(a)

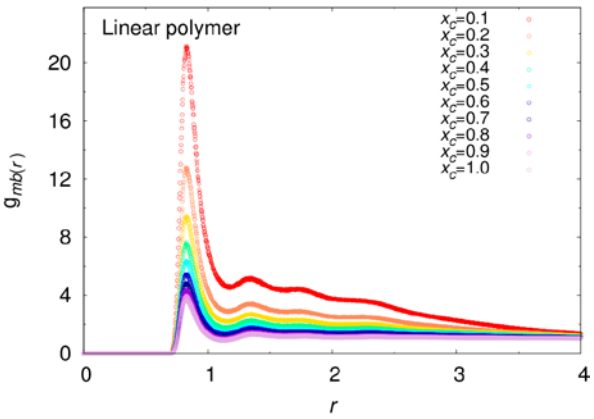

(b)

General picture of co-nonsolvency for linear and ring polymers

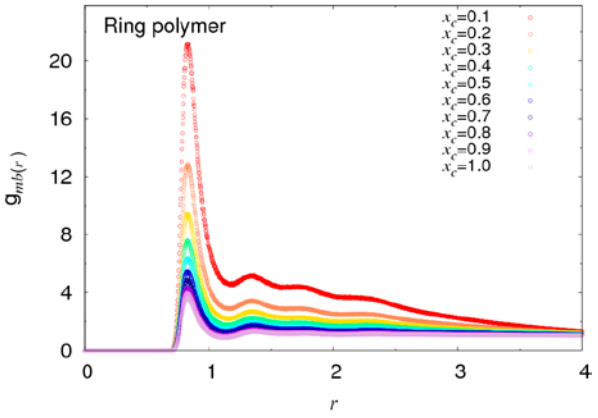

Figure 5. Radial distribution functions for monomer-better solvent pair as a function of pair distance for (a) linear and (b) ring polymer systems of *N*=30. Different colors represent different better solvent concentrations.

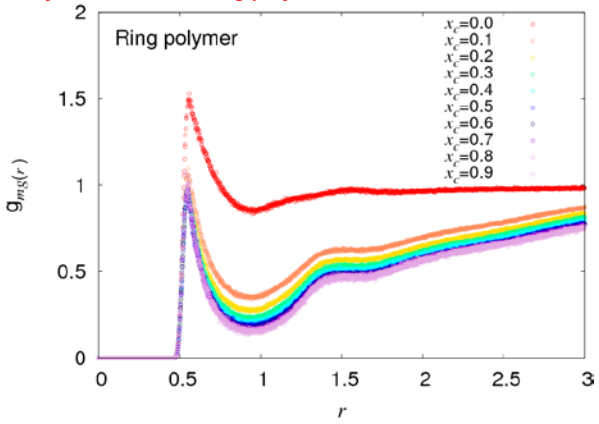

Figure 6. Radial distribution functions for monomer-better solvent pair as a function of pair distance for (a) linear and (b) ring polymer systems of *N*=30. Different colors represent different better solvent concentrations.

According to reversible work theorem, radial distribution function is linked to the potential of mean force such that:[21]

$$g(r) = e^{-\beta u_{eff}(r)}. \tag{11}$$

Considering radial distribution functions in Figs. 4 and 5, we can state that the effective potential between a monomer and solvents differs the solvent composition changes. In order to qualitatively observe the changes of effective potential between pairs, we calculate Kirkwood-Buff (KB) integrals. This integral is an indicator of affinity between two types of molecules, which is related to the excluded volume of a specific pair (Eqn. (5)), such that:[22,23]

$$\begin{aligned} G_{ij} &= 4\pi \int_0^\infty [g_{ij}(r) - 1] r^2 dr \\ &= 4\pi \int_0^\infty [e^{-\beta U_{eff}(r)} - 1] r^2 dr \\ &= 4\pi \int_0^\infty f_{ij}(r) r^2 dr = -v_{ex,ij} \end{aligned} \tag{12}$$

(a)

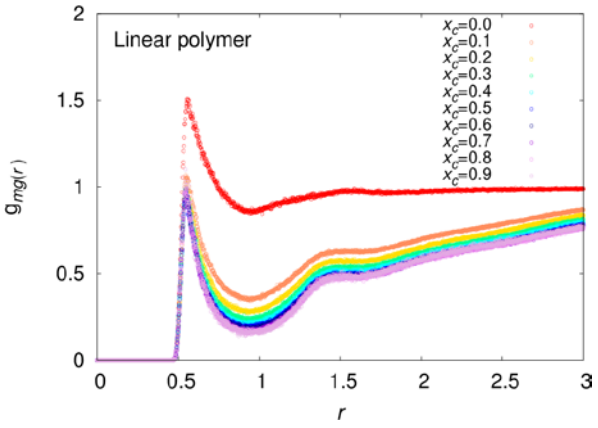

(b)

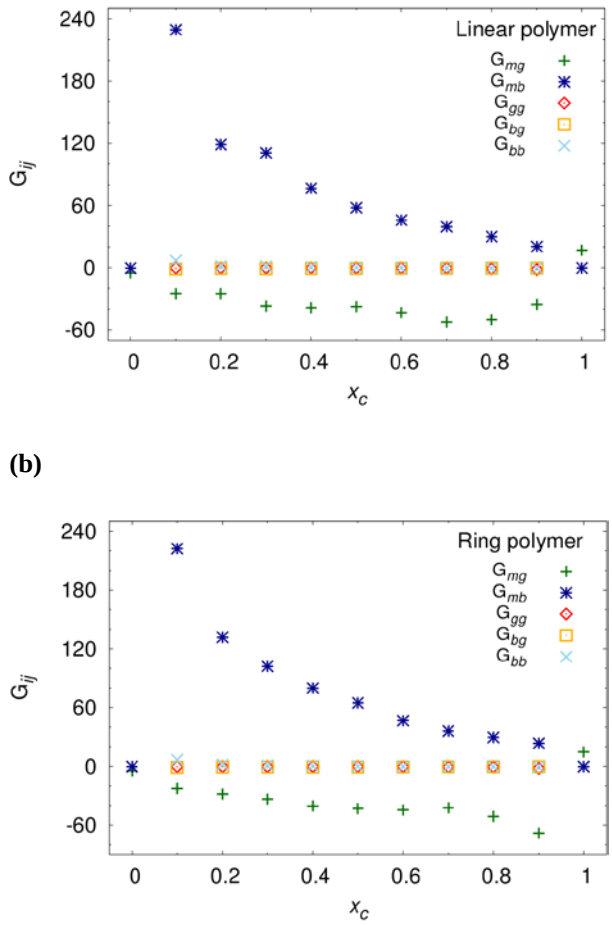

(b)

Figure 7. Kirkwood-Buff integrals, G_{ij}, between different solution compositions as a function of cosolvent molar fraction for (a) linear and (b) ring polymers of N_I=30. G_{ij} is calculated by integrating Mayer's *f*-function in Eqn. (12)

Figure 7 represents KB integral between a monomer and a better solvent, G_{mb}. It is noticeable that G_{mb} rapidly changes with increasing x_c and has a maximum at x_c=0.1. This reflects the excluded volume between this pair is smallest in this solvent composition and attraction between this pair is strongest in this condition. As the fraction of the cosolvent increases, G_{mb} gradually decreases as well as affinity of polymer-better solvent, which leads to re-opening of the polymer configuration. The small difference of bridging fractions between linear and ring polymers seems to be caused by the difference in G_{mg} at large x_c. Effective interaction between a monomer and a good solvent for a ring at large x_c is more repulsive than the linear counterpart. We can argue that relatively small number of backbone sites are available to be occupied by good solvents due to the ring already forms a loop.

According to the KB theory, the slope of μ_p with respect to cosolvent fraction is given by:

$$\left(\frac{\partial \mu_p}{\partial x_c}\right)_{p,T} = \frac{G_{mg} - G_{mb}}{1 - x_c(G_{bg} - G_{bb})}. \quad (13)$$

By integrating Eqn. (13), we calculate a chemical potential of a polymer as a function of x_c (Fig. 8). It should be noted that even if the polymer is collapsed in mixed solvents, it is well solvated by solvent molecules represented by negative chemical potential in all solvent compositions. This finding breaks the traditional picture of the relation between the solvent quality and the polymer conformation. This is also in good agreement with the analytical result, which can be calculated by differentiating Eqn. (9) with respect to x_c, such that:

$$\mu_p \sim -mkT\phi_B \ln\left\{1 + \phi_B^{m/2}\left(\frac{x_c}{x_c^{**}}\right)^{1/2} + \left(\frac{x_c}{x_c^{*}}\right)\right\}. \quad (14)$$

Moreover, negative values of polymer chemical potentials in all solvent compositions indicate that the coil-globule-coil transition is totally controlled by a thermodynamic free energy. The coil-globule transition resembles the first-order thermodynamic phase transition in which the enthalpic stabilization by bridging structure is dominant. Reentrance from globule to coil structures is a continuous transition where the stabilization energy from the bridging structure is no longer advantageous and the polymer again follows SAW statistics.

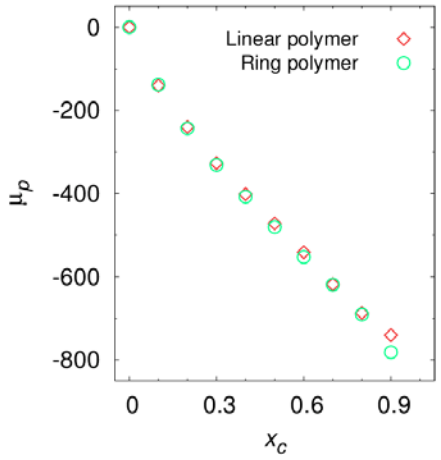

Figure 8. Chemical potential of a single monomer as a function of cosolvent mole fraction x_c for linear (squares) and ring (circles) polymers.

Conclusion

In this work, we performed Monte Carlo simulations to understand physical origin of the coil-globule-coil transition of linear and ring polymer solutions. Our simulation results reveal that the co-nonsolvency is originated from the local affinity between a polymer and a cosolvent, which makes a

bridging structure. Modified adsorption model considers the local density fluctuation of solvent molecules to explain the simulation results. Using this theory, we find that the coil-globule-coil transition is a thermodynamic transition controlled by thermodynamic free energy. We also show that rings have higher looping probability than linear polymers, thus the bridging fraction remains higher at large x_c. The ring polymer has smaller free energy penalty for looping than linear polymer, and the adsorption theory succesfully describes the high bridging fraction for rings. From this work, we provide generic understanding of polymer solution system for ring and linear polymer.

Acknowledgments. This work has been supported by the project EDISON (EDucation-research Integration through Simulation On the Net), Chemistry.

References

1. Cohen-Stauart, W. T. S. Huck, J. Genzer, M. Müller, C. Ober, M. Stamm, G. B. Sukhorukov, I. Szleifer, V. V. Tsukruk, M. Urban, F. Winnik, *Nat. Mater*. **2010**, *9*, 101.
2. Jeffrey R. Capadona, Kadhiravan Shanmuganathan,Dustin J. Tyler, Stuart J. Rowan, Christoph Weder, *Science.* **2008**, *319*, 1370.
3. S. Cui, X. Pang, S. Zhang, Y. Yu, H. Ma, X. Zhang, *Langmuir*, **2012**, *28*, 5151
4. S. de Beer, E. Kutnyanszky, P. M. Schön, G. J. Vansco, M. H. Müser, *Nat. Commun.* **2014**, *5*, 3781
5. Howard G. Schild, M. Muthukumar, David A. Tirrell, *Macromolecules* **1990**, *24*, 948.
6. Fumihiko Tanaka, Tsuyoshi Koga, *Phys. Rev. Lett.* **2008**, *101*, 028302
7. J. J. Magda, G. H. Fredrickson, R. G. Larson, E. Helfand, *Macromolecules*, **1988**, *21*, 726
8. J. Walter, J. Sehrt, J. Vrabec, H. Hasse, *J. Phys. Chem. B*, **2012**, *116*, 5251-5259
9. Debashish Mukheriji, Carlos M. Marques, Kurt Kremer, Nat. Commun. **2014**, *5*, 4882.
10. D. Mukherji, K. Kremer, *Macromolecules*, **2013**, *46*, 9158-9163
11. D. Mukherji, C. M. Marques, T. Stuehn, K. Kremer, *J. Chem. Phys.* **2015**, *142*, 114903
12. M. E. Cates, J. M. Deutsch, *J. Phys. France*, **1986**, *47*, 2121-2128
13. M. Rubinstein, *Phys. Rev. Lett.* **1986**, *57*, 3023-3026
14. J. D. Halverson, W. B. Lee, G. s. Grest, A. Y. Grosberg, K. Kremer, *J. Chem. Phys.* **2011**, *134*, 204904
15. E. Lee, S. Kim, Y. Jung, *Macrmol. Rapid Commun.* **2015**, *36*, 1115-1121
16. E. Lee, Y. Jung, *Soft Matter*, **2015**, *11*, 6018-6028
17. Z. –C. Yan, S. Costanzo, Y. Jeong, T. Chang, D. Vlassopoulos, *Macromolecules*, **2016**, 49, 1444
18. Kurt Kremer, *J. Chem. Phys.* **1990**, *92*, 5057.
19. Walter. J., Sehrt. J, Vrabec. J, Hasse. H., *J. Phys. Chem. B.* **2012**, *116*, 5251.
20. Michael Rubinstein, Ralph H. Colby, *Polymer physics*, Oxford University press, New York, **2003**, p. 102.
21. David Chandler, *Introduction to Modern Statistical Mechanics*, Oxford University Press, Newyork, **1987**, p. 201
22. John G. Kirkwood, Frank P. Buff, *J. Chem. Phys.* **1951**, *19*, 774.
23. Michael Rubinstein, Ralph H. Colby, *Polymer physics*, Oxford University press, New York, **2003**, p. 99.